

Distribution of velocities in an avalanche, and related quantities: Theory and numerical verification

ALEJANDRO B. KOLTON¹, PIERRE LE DOUSSAL² and KAY JÖRG WIESE²

¹ *Centro Atómico Bariloche and Instituto Balseiro, Comisión Nacional de Energía Atómica (CNEA), Consejo Nacional de Investigaciones Científicas y Técnicas (CONICET), Universidad Nacional de Cuyo (UNCUYO) Av. E. Bustillo 9500, R8402AGP San Carlos de Bariloche, Río Negro, Argentina*

² *Laboratoire de Physique de l'Ecole Normale Supérieure, ENS, Université PSL, CNRS, Sorbonne Université, Université Paris-Diderot, Sorbonne Paris Cité - 24 rue Lhomond, 75005 Paris, France*

received 18 April 2019; accepted in final form 16 August 2019

published online 11 September 2019

PACS 64.60.av – Cracks, sandpiles, avalanches, and earthquakes

PACS 68.35.Rh – Phase transitions and critical phenomena

PACS 05.70.Jk – Critical point phenomena

Abstract – We study several probability distributions relevant to the avalanche dynamics of elastic interfaces driven on a random substrate: The distribution of size, duration, lateral extension or area, as well as velocities. Results from the functional renormalization group and scaling relations involving two independent exponents, roughness ζ , and dynamics z , are confronted to high-precision numerical simulations of an elastic line with short-range elasticity, *i.e.*, of internal dimension $d = 1$. The latter are based on a novel stochastic algorithm which generates its disorder on the fly. Its precision grows linearly in the time discretization step, and it is parallelizable. Our results show good agreement between theory and numerics, both for the critical exponents as for the scaling functions. In particular, the prediction $\alpha = 2 - \frac{2}{d+\zeta-z}$ for the velocity exponent is confirmed with good accuracy.

Copyright © EPLA, 2019

Introduction. – Disordered systems, when driven slowly or via a small kick, do not respond smoothly, but in a bursty way. An example are elastic manifolds, or more specifically elastic strings, subject to a random potential. An example for the global velocity as a function of time is shown in fig. 1. At $t = 0$, the system received a small kick. The velocity as a function of time t then performs a random walk, which terminates at a precise moment in time. Driving the system adiabatically slowly, it is at rest for most of the time, interceded with jerky motion as the one shown in fig. 1. Each such event is called an avalanche. Avalanches are ubiquitous, found in earthquakes in geoscience [1], Barkhausen noise [2,3] in dirty disordered magnets, contact-lines on a disordered substrate [4], and many more.

The theory has been developed for many years, starting with phenomenological and mean-field arguments [5,6]. In the context of magnets, a more systematic approach was proposed by Alessandro, Beatrice, Bertotti, and Montorsi (ABBM) [7,8], who reduced the equation of motion for a magnetic domain wall to a *single degree of freedom*, subject to a random force modeled as a random walk. It was only

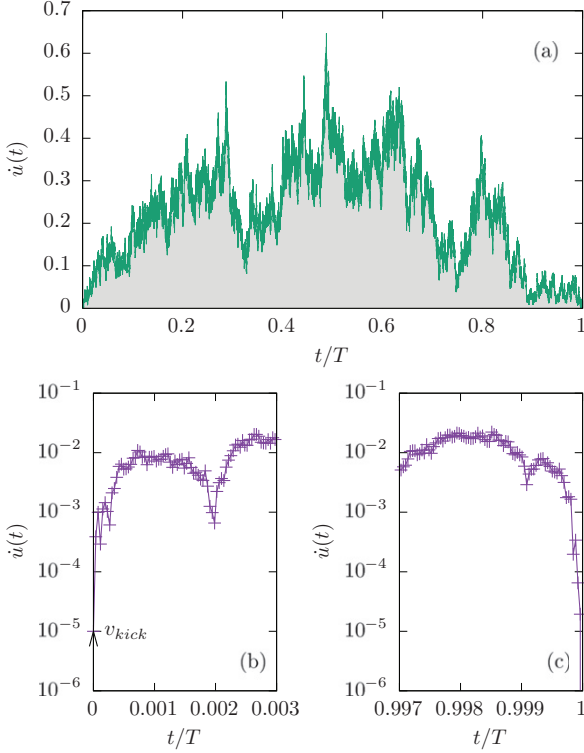
realized later [9] that the Brownian force model (BFM) is the correct mean-field theory for the avalanche dynamics. In contrast to the ABBM or similar mean-field models, which have a single degree of freedom, the BFM is an extended model, in which each degree of freedom, *i.e.*, each piece of the elastic manifold, sees an independent random force, which itself is a random walk. In [9] it was shown that its center of mass is the same stochastic process as the single degree of freedom of the ABBM model.

The BFM is the starting point for a field theory of elastic manifolds subject to short-ranged disorder. It allows us to calculate a plethora of observables beyond pure scaling exponents, as, *e.g.*, the full size distribution [10–12], the velocity distribution [9,13], and the temporal [14,15] or spatial shape [16–19] of an avalanche.

In this letter we study numerically, and compare to the field theory, the distributions of the duration T of an avalanche, its size $S = \int_0^T \dot{u}(t)dt$, its velocity \dot{u} , and extension ℓ , defined as the number of interface points that actively participated in an avalanche. We briefly review the corresponding scaling relations, and then confront them to large-scale numerical simulations. The latter have been

Table 1: Left: scaling relations for short-range (SR) and long-range (LR) elasticity. Right: critical exponents obtained via the scaling relations using standard values for ζ and z [20–23].

	$P(S)$	$P(T)$	$P(\dot{u})$	$P(V)$		d	ζ	z	τ	α	a	k_V
	$S^{-\tau}$	$T^{-\alpha}$	\dot{u}^{-a}	V^{-k_V}		1	5/4	10/7	10/9	47/40	-10/23	1.25
SR	$\tau = 2 - \frac{2}{d+\zeta}$	$\alpha = 1 + \frac{d-2+\zeta}{z}$	$a = 2 - \frac{2}{d+\zeta-z}$	$k_V = 2 - \frac{2-\zeta}{d}$	SR	2	0.75	1.56	1.27	1.48	0.32	1.38
						3	0.35	1.75	1.40	1.77	0.75	1.45
LR	$\tau = 2 - \frac{1}{d+\zeta}$	$\alpha = 1 + \frac{d-1+\zeta}{z}$	$a = 2 - \frac{1}{d+\zeta-z}$	$k_V = 2 - \frac{1-\zeta}{d}$	LR	1	0.39	0.77	1.28	1.51	0.39	1.39

Fig. 1: (a) The velocity as a function of time t for one avalanche of duration T . (Parameters are $T = 26.2$, $A = 10$, $L = 64$, $m = 1$.) Zooms of the departure (b), and ending (c) of the avalanche. The arrow in (b) indicates the magnitude v_{kick} of the uniform velocity kick triggering the avalanche.

possible through the development of a novel powerful algorithm which generates the disorder on the fly by accurately solving an extension of the BFM to model short-ranged disorder.

Definition of the model. – Consider the overdamped equation of motion for a manifold in a random-field environment,

$$\partial_t u_{x,t} = \partial_x^2 u_{x,t} + F(x, u_{x,t}) + m^2(w_t - u_{x,t}). \quad (1)$$

The manifold is trapped in a harmonic potential of width m^2 , and position w_t . The well is moved slowly, either via $w_t = vt$ in the limit $v \rightarrow 0^+$ (constant-velocity driving), or by augmenting w by a small amount δw at discrete times t (kick driving). F is a short-ranged correlated

random force, which will be specified below. Equation (1) provides a well-defined framework to study avalanches, both in the field theory [9,13–15,24,25], as for simulations [26–32]. Indeed, the velocity as a function of time performs a burst-like evolution, with a well-defined beginning and end, see fig. 1(a), separated by periods without activity (not shown).

Scaling relations. – The theory of the depinning transition of interfaces [20,33–38] introduces two independent critical exponents, the roughness exponent ζ , and the dynamic exponent z . Within the field theory developed in [9,13–15,24,25] no independent exponent is required to describe avalanches. As a consequence, their exponents are given by scaling relations, together with the requirement of the existence of a massless field theory [24], a generalization of the arguments of ref. [34]. Consider the PDF $P_{\delta w}(S)$ of the total size S of the avalanche following a small kick δw . Its large-size cutoff $S_m \sim m^{-(d+\zeta)}$ is defined through the ratio of its first two moments [12],

$$S_m = \frac{\langle S^2 \rangle}{2\langle S \rangle}. \quad (2)$$

The PDF reads, for S larger than a microscopic cutoff,

$$P_{\delta w}(S) \simeq \frac{\langle S \rangle}{S_m^2} p(S/S_m), \quad \langle S \rangle = \delta w L^d, \quad (3)$$

where $p(s)$ is a universal scaling function with $p(s) \sim s^{-\tau}$ at small s , defining the size exponent τ . Existence of a massless field theory imposes that the avalanche density per unit applied force, $\rho_f(S) = \lim_{\delta w \rightarrow 0} \frac{1}{m^2 \delta w} P_{\delta w}(S)$, has a finite limit for $m \rightarrow 0$. This requires $m^{-2} S_m^{\tau-2}$ to be independent of m at small m , hence $\tau = 2 - \frac{2}{d+\zeta}$, recovering the value of Narayan and Fisher [34]. The exponents for the avalanche duration T , or lateral size ℓ are then obtained by writing $P_{\delta w}(S)dS = P_{\delta w}(T)dT$, and using the appropriate scaling relations between S , m and T , leading to the results in table 1, where numerical values are given as well. We also consider the (spatially integrated) velocity at time t after the kick, $\dot{u}(t) = \int d^d x \partial_t u_{x,t}$. The PDF of the total velocity $\dot{u} = \dot{u}(t)$ is obtained by considering many successive kicks and sampling the time t uniformly. Its associated density is $\rho_f(\dot{u}) \sim \int dt \rho_f(\dot{u}(t))$. By scaling it takes at small \dot{u} the form $\rho_f(\dot{u}) = \frac{L^d}{m^2 v_m^2} (v_m/\dot{u})^a$, where a is the velocity exponent, $v_m = S_m/\tau_m$ and $\tau_m \sim m^{-z}$ is

the large-time cutoff. The requirement of a massless limit implies

$$a = 2 - \frac{2}{d + \zeta - z}, \quad (4)$$

a main prediction of ref. [24], in agreement with the ϵ expansion of ref. [13], and which we test numerically below.

The algorithm: theory. – Specifying a realization of the disorder force F over a range of u sufficiently large, eq. (1) can be integrated numerically, allowing one to access all quantities of interest. This method was used extensively (see [30–32] for a review and recent applications). Here, we follow a different strategy: We develop a stochastic algorithm to solve a dynamical system in the same universality class. As we discuss later, this method presents some important advantages over the standard one based on eq. (1), in particular for observables related to the avalanche duration.

We first state that the equation of motion of an elastic manifold due to short-ranged disorder-forces can be generated by the following set of equations (with an arbitrary constant A) [25,39]:

$$\partial_t \dot{u}_{x,t} = \partial_x^2 \dot{u}_{x,t} + \partial_t \mathcal{F}_{x,t} + m^2(v - \dot{u}_{x,t}), \quad (5)$$

$$\partial_t \mathcal{F}_{x,t} = -A \mathcal{F}_{x,t} \dot{u}_{x,t} + \sqrt{2A \dot{u}_{x,t}} \xi(x, t), \quad (6)$$

$$\langle \xi(x, t) \xi(x', t') \rangle = \delta(x - x') \delta(t - t'). \quad (7)$$

The first line is the time derivative of eq. (1), its time integral allowing to reconstruct $u(x, t)$. The second line is the update of the random force, which we show now to be statistically equivalent to a *quenched* random force $F(x, u)$. To this purpose, rewrite $\mathcal{F}_{x,t}$ as a function of x and $u_{x,t}$, $\mathcal{F}_{x,t} \equiv F(x, u_{x,t})$. This yields for each x an evolution equation for $F(x, u)$,

$$\partial_u F(x, u) = -A F(x, u) + \sqrt{2A} \eta(x, u), \quad (8)$$

$$\langle \eta(x, u) \eta(x', u') \rangle = \delta(x - x') \delta(u - u'). \quad (9)$$

Note that this change of variables is possible since $\dot{u}_{x,t} \geq 0$, a property which holds in the zero-temperature sliding state for any $(d + 1)$ -dimensional elastic manifold with a convex elastic energy in a quenched potential [40,41]. The solution to this equation is

$$\overline{F(x, u) F(x', u')} = \delta(x - x') e^{-A|u' - u|}. \quad (10)$$

The microscopic disorder force-force correlator thus is

$$\Delta(u - u') = e^{-A|u' - u|}. \quad (11)$$

It is short-ranged, and *microscopically rough*. Note that computationally it is more convenient and efficient to update the forces as a function of time than having to generate an independent set of forces as a function of u , and refine the latter as necessary. As can be seen from eq. (6), fixing a time discretisation step δt implies a u discretisation step of $\delta u = \dot{u} \delta t$, which becomes more refined when the velocity is small, an important advantage. Finally,

dealing with a white noise $\xi(x, t)$ is both numerically and analytically advantageous, and allows one to connect to other seemingly unrelated stochastic problems [39,42].

Generating a microscopically rough disorder “on the fly”, with a prescribed correlation length, is one of the main advantages of our algorithm. It allows us to drive the elastic system quasistatically, to generate a large number of stationary avalanches in a long run (avoiding storage of a large disorder configuration), and to compute precisely the spatio-temporal extent of an avalanche in the continuous displacement model of eq. (1). To illustrate the method, in fig. 1(a) we show the calculated center-of-mass (COM) velocity of a typical avalanche with a well-defined total duration T , while in figs. 1(b), (c), we zoom in on the COM velocity near its beginning ($0 < t/T \ll 1$) and end ($1 - t/T \ll 1$). At the departure, in fig. 1(b), a small uniform kick in the velocity ($v_{\text{kick}} = 10^{-5}$) triggers the avalanche, and a sharp increase in the COM velocity is observed, reaching 10^4 times the kick velocity in fig. 1. Note that since the total advance $\langle S \rangle$ is proportional to the kick, there are many more avalanches which decay rather quickly; these do not contribute to quantities we are interested in, as the size ratio $\langle S^2 \rangle / \langle S \rangle$. As a consequence, the pulse driving of magnitude v_{kick} is fairly quasistatic. Finally, the end of the avalanche, shown in fig. 1(b), is clearly observed as a sharp decrease in the COM velocity. These features of our algorithm are particularly important to precisely measure the duration T . It is worth noting that the smooth pinning potentials normally used in numerical simulations of eq. (1) require to perform an accurate, and expensive, time integration of eq. (1), which, in turn, displays a strong *critical slowing-down* near both avalanche extremes. This is *not a collective effect*, and requires one to go to huge avalanches, or introduce an artificial threshold for the velocity, which, in turn, introduces spurious avalanche correlations [43]. Our stochastic method is by construction free of these artifacts.

The remaining problem is how to solve efficiently the stochastic equations (5), (6). A first approach is to discretize time in steps of size δt , yielding

$$\begin{aligned} \dot{u}_{t+\delta t} - \dot{u}_t &= \mathcal{F}_{t+\delta t} - \mathcal{F}_t + O(\delta t) \\ &= \sqrt{2A \dot{u}_t \delta t} \xi_t + O(\delta t), \end{aligned} \quad (12)$$

where ξ_t is a normal-distributed Gaussian random variable with mean $\langle \xi_t \rangle = 0$, and variance $\langle \xi_t \xi_{t'} \rangle = \delta_{t,t'}$. This is the most efficient approach as long as one can use relatively large δt . Here we are interested in the limit of $\delta t \rightarrow 0$, thus the appearance of $\sqrt{\delta t}$ in front of the noise term implies a rather slow convergence.

The algorithm: an improved solver. – The idea is to first solve analytically the (for small δt) most singular term in eqs. (5) and (6), equivalent to the random process

$$\partial_t \dot{u}_t = \sqrt{2A \dot{u}_t} \xi(t) \quad (13)$$

with absorbing boundary conditions at $\dot{u} = 0$ for a finite interval δt , and only later add the drift terms proportional

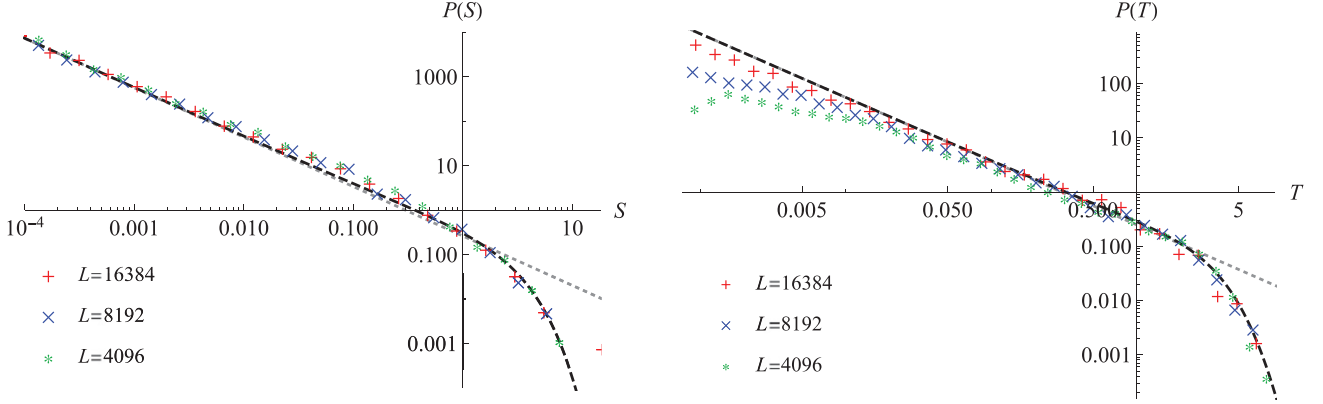


Fig. 2: Left: the rescaled distribution of size $P(S)$. To avoid system-spanning avalanches, the ratio $Lm = 10$ is kept fixed. The black dashed line is the 1-loop result (12) of ref. [44], the gray dotted line the pure power law. Right: the same for the duration distribution $P(T)$. The analytical result is given in eqs. (3.113)–(3.116) of ref. [25] and in ref. [15]. Note that in all of our curves there is no fitting parameter, as all scales are measured. As an example, for $P(S)$ one measures the first two moments $\langle S \rangle$ and $\langle S^2 \rangle$, which then defines the scale $S_m := \langle S^2 \rangle / (2\langle S \rangle)$. Rescaling all data by S_m , the ensuing scaling function plotted above has no adjustable parameter left.

to δt . Following [45], we first write the analytic solution of the corresponding Fokker-Planck equation

$$P(\dot{u}, t) = \delta(\dot{u}) \exp\left(-\frac{\dot{u}_0}{At}\right) + \frac{\exp\left(-\frac{\dot{u}_0 + \dot{u}}{At}\right)}{At} \sqrt{\frac{\dot{u}_0}{\dot{u}}} I_1\left(\frac{2\sqrt{\dot{u}_0 \dot{u}}}{At}\right), \quad (14)$$

where I_1 is the Bessel- I function of the first kind. It can be expressed as a series

$$P(\dot{u}, t) = \sum_{n=0}^{\infty} p_n \frac{1}{At} P_n\left(\frac{\dot{u}}{At}\right) \quad (15)$$

with

$$p_n = \frac{\left(\frac{\dot{u}_0}{At}\right)^n \exp\left(-\frac{\dot{u}_0}{At}\right)}{n!}, \quad (16)$$

$$P_0(y) = \delta(y), \quad (17)$$

$$P_n(y) = \frac{y^{n-1} \exp(-y)}{(n-1)!}, \quad n \geq 1. \quad (18)$$

The algorithm consists of two steps: First draw a random number n from a Poisson distribution with parameter $\frac{\dot{u}_0}{At}$. Second draw a random number y from a Gamma distribution with the (previously determined) parameter n . This yields

$$\dot{u}_{t+\delta t} = \dot{u}_t + Ay \delta t, \quad (19)$$

to which are added the drift terms proportional to δt .

Our method has the drawback that performing a single time step is computationally more costly than the direct integration of eq. (1) with smooth pinning potentials, or the direct integration of eq. (12). Thus, we are far from the sizes of ref. [29], where parallelization allowed the authors to reach size $L = 2^{25}$, while in our work the maximum is $L = 2^{14}$. Large sizes are needed to obtain purely geometrical properties such as the roughness exponent and related

quantities. Velocity observables or time-dependent properties, such as the avalanche duration, are more efficiently targeted using the present algorithm.

Results: size and duration distributions. – Our simulations are performed in dimension $d = 1$. In fig. 2, we report our findings for the avalanche size and duration distributions, both known analytically from the $\epsilon = 4 - d$ expansion [12,15,25]. The size distribution was also checked numerically [27]. One extends the definitions of eqs. (2) and (3) to observables \mathcal{O} such as the duration T and extension ℓ (see below) by writing the probability distribution function (PDF)

$$P_{\delta w}(\mathcal{O}) = \frac{\langle \mathcal{O} \rangle}{\mathcal{O}_m^2} p\left(\frac{\mathcal{O}}{\mathcal{O}_m}\right), \quad (20)$$

where $\mathcal{O}_m = \frac{\langle \mathcal{O}^2 \rangle}{2\langle \mathcal{O} \rangle}$ is the characteristic large-scale cutoff, and $p(x)$ is a universal function depending only on d and \mathcal{O} , such that $\int_0^\infty dx x p(x) = 1$, $\int_0^\infty dx x^2 p(x) = 2$. It is this function $p(x)$ which is plotted in figs. 2 and 4 from our simulation, (denoted there by $P(x)$) and compared to its prediction from the ϵ expansion (via an extrapolation to $\epsilon = 3$). While the scaling relations using $\zeta = 5/4$ and $z = 10/7$ predict a size exponent $\tau = 1.11$ and a duration exponent $\alpha = 1.17$, see table 1, our best fits are

$$\tau = 1.2 \pm 0.2, \quad (21)$$

$$\alpha = 1.1 \pm 0.15. \quad (22)$$

Velocity distribution. – For the center of mass, the velocity distribution $P(\dot{u})$ is predicted to scale as

$$P(\dot{u}) \sim \dot{u}^{-a}, \quad (23)$$

with a very large exponent $a = 1$ for the BFM and the ABBM model (see fig. 3). On the other hand, the scaling

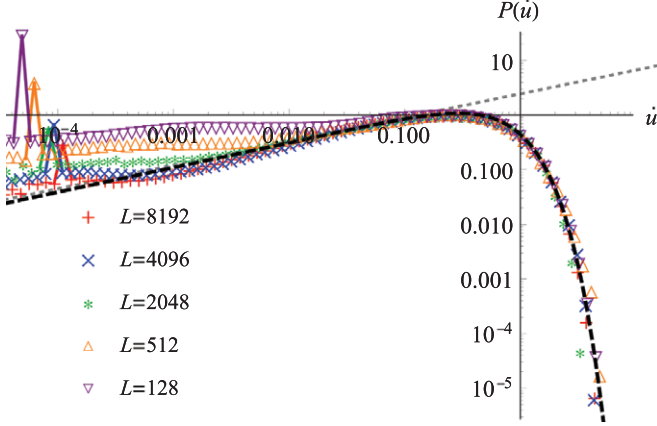


Fig. 3: The center-of-mass velocity distribution $P(\dot{u})$. The weight of the peak at $\dot{u} = v_{\text{kick}}$ is $\frac{\delta t}{T} \sim L^{-z} \sim m^z$, where T is the duration of an avalanche and δt the time discretization step. The analytic result (black dashed line) is from eq. (385) of ref. [13], the dotted gray line the pure power law $P(\dot{u}) \sim \dot{u}^{-a}$, with a given in eq. (4). As noted in the caption of fig. 2, there is no adjustable (fitting) parameter, thus convergence to the theory including all scales is read off from the plot.

relation (4) predicts a negative exponent $a = -0.45$ in dimension $d = 1$, a quite dramatic deviation from the value of the BFM and MF. Our simulations confirm this negative value, yielding

$$a = -0.45 \pm 0.05. \quad (24)$$

Distribution of spatial extensions. – We finally consider the spatial extension ℓ of an avalanche. Using that $P(\ell)d\ell = P(S)dS$, and $S \sim \ell^{d+\zeta}$, we get

$$P(\ell) \sim \ell^{-k}, \quad k = d - 1 + \zeta \xrightarrow{d=1} \zeta = 1.25. \quad (25)$$

Our numerical data shown in fig. 4 are in agreement with this scaling relation, yielding

$$k = 1.25 \pm 0.05. \quad (26)$$

In higher dimensions, the lateral extension of an avalanche is difficult to define, whereas its volume is well defined. Using scaling arguments equating $P(V)dV = P(S)dS$, $S \sim \ell^{d+\zeta}$, and $V \sim \ell^d$ we find

$$P(V) \sim V^{-k_V}, \quad (27)$$

$$k_V = 2 - \frac{2 - \zeta}{d}. \quad (28)$$

Explicit values are given in table 1.

Conclusion. – We confronted theoretical results for the distributions of avalanche size, duration, and velocity with numerical simulations. We confirm the theoretical results based on scaling arguments, and functional RG calculations to 1-loop order. Our comparison goes beyond exponents, validating the full 1-loop scaling functions.

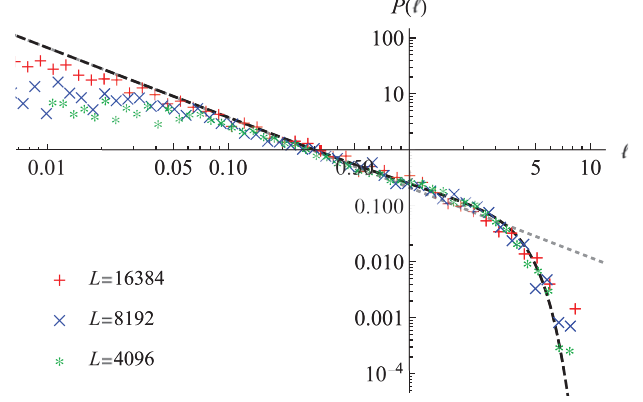


Fig. 4: The distribution of lateral sizes $P(\ell)$. In the absence of analytic results for the scaling function, we use the relation $P(\ell)d\ell = P(S)dS$, and $S = \ell^{d+\zeta}$ to infer the latter (black dashed line). A pure power law $P(S) \sim S^{-k}$ is given as a gray dotted line.

The model and algorithm proposed here can be generalized to arbitrary dimension and long-range interactions. It is computationally more demanding than the standard depinning model due to the presence of multiplicative noise, but it has the advantage to compute more precisely the spatio-temporal extent of an avalanche and to reach the regime of adiabatic driving. It avoids the difficulties and artifacts associated with velocity thresholding. In addition, as its microscopic disorder has the statistics of a random walk, it is readily connected to the BFM.

We thank A. DOBRINEVSKI for very useful discussions. PLD and KJW acknowledge support from PSL grant ANR-10-IDEX-0001-02-PSL and thank KITP for hospitality and support in part under Grant NSF PHY11-25915. ABK acknowledges support from Grants PICT2016-0069/FONCyT and UNCuyo C017, from Argentina.

REFERENCES

- [1] GUTENBERG B. and RICHTER C. F., *Bull. Seismolo. Soc. Am.*, **46** (1956) 105.
- [2] BARKHAUSEN H., *Phys. Z.*, **20** (1919) 401.
- [3] CIZEAU P., ZAPPERI S., DURIN G. and STANLEY H., *Phys. Rev. Lett.*, **79** (1997) 4669.
- [4] LE DOUSSAL P., WIESE K. J., MOULINET S. and ROLLEY E., *EPL*, **87** (2009) 56001 (arXiv:0904.4156).
- [5] BULDYREV S. V., BARABASI A. L., CASERTA F., HAVLIN S., STANLEY H. E. and VICSEK T., *Phys. Rev. A*, **45** (1992) R8313.
- [6] FISHER D. S., *Phys. Rep.*, **301** (1998) 113.
- [7] ALESSANDRO B., BEATRICE C., BERTOTTI G. and MONTORSI A., *J. Appl. Phys.*, **68** (1990) 2901.
- [8] ALESSANDRO B., BEATRICE C., BERTOTTI G. and MONTORSI A., *J. Appl. Phys.*, **68** (1990) 2908.
- [9] LE DOUSSAL P. and WIESE K. J., *EPL*, **97** (2012) 46004 (arXiv:1104.2629).

- [10] LE DOUSSAL P. and WIESE K. J., *Phys. Rev. E*, **85** (2011) 061102 (arXiv:1111.3172).
- [11] LE DOUSSAL P. and WIESE K. J., *Phys. Rev. E*, **82** (2010) 011108 (arXiv:0908.4001).
- [12] LE DOUSSAL P. and WIESE K. J., *Phys. Rev. E*, **79** (2009) 051106 (arXiv:0812.1893).
- [13] LE DOUSSAL P. and WIESE K. J., *Phys. Rev. E*, **88** (2013) 022106 (arXiv:1302.4316).
- [14] DOBRINEVSKI A., LE DOUSSAL P. and WIESE K. J., *Phys. Rev. E*, **85** (2012) 031105 (arXiv:1112.6307).
- [15] DOBRINEVSKI A., LE DOUSSAL P. and WIESE K. J., *Avalanches beyond mean-field: durations and shape*, in preparation.
- [16] THIERY T., LE DOUSSAL P. and WIESE K. J., *J. Stat. Mech.*, **2015** (2015) P08019 (arXiv:1504.05342).
- [17] DELORME M., LE DOUSSAL P. and WIESE K. J., *Phys. Rev. E*, **93** (2016) 052142 (arXiv:1601.04940).
- [18] ARAGON L. E., KOLTON A. B., LE DOUSSAL P., WIESE K. J. and JAGLA E., *EPL*, **113** (2016) 10002 (arXiv:1510.06795).
- [19] ZHU Z. and WIESE K. J., *Phys. Rev. E*, **96** (2017) 062116 (arXiv:1708.01078).
- [20] LESCHHORN H., NATTERMANN T., STEPANOW S. and TANG L.-H., *Ann. Phys. (Berlin)*, **509** (1997) 1 (arXiv:cond-mat/9603114).
- [21] DÜMMER O. and KRAUTH W., *Phys. Rev. E*, **71** (2005) 061601.
- [22] FERRERO E. E., BUSTINGORRY S. and KOLTON A. B., *Phys. Rev. E*, **87** (2013) 032122 (arXiv:1211.7275).
- [23] GRASSBERGER P., DHAR D. and MOHANTY P. K., *Phys. Rev. E*, **94** (2016) 042314.
- [24] DOBRINEVSKI A., LE DOUSSAL P. and WIESE K. J., *EPL*, **108** (2014) 66002 (arXiv:1407.7353).
- [25] DOBRINEVSKI A., *Field theory of disordered systems – avalanches of an elastic interface in a random medium*, PhD Thesis, ENS Paris (2013), arXiv:1312.7156.
- [26] ROSSO A., LE DOUSSAL P. and WIESE K. J., *Phys. Rev. B*, **75** (2007) 220201 (cond-mat/0610821).
- [27] ROSSO A., LE DOUSSAL P. and WIESE K. J., *Phys. Rev. B*, **80** (2009) 144204 (arXiv:0904.1123).
- [28] KOLTON A. B., SCHEHR G. and LE DOUSSAL P., *Phys. Rev. Lett.*, **103** (2009) 160602 (arXiv:0906.2494).
- [29] FERRERO E. E., BUSTINGORRY S. and KOLTON A. B., *Phys. Rev. E*, **87** (2013) 032122.
- [30] FERRERO E. E., BUSTINGORRY S., KOLTON A. B. and ROSSO A., *C. R. Phys.*, **14** (2013) 641.
- [31] KOLTON A. B. and JAGLA E. A., *Phys. Rev. E*, **98** (2018) 042111.
- [32] CAO X., BOUZAT S., KOLTON A. B. and ROSSO A., *Phys. Rev. E*, **97** (2018) 022118.
- [33] NATTERMANN T. *et al.*, *J. Phys. II*, **2** (1992) 1483.
- [34] NARAYAN O. and FISHER D. S., *Phys. Rev. B*, **46** (1992) 11520.
- [35] NARAYAN O. and FISHER D. S., *Phys. Rev. B*, **48** (1993) 7030.
- [36] FISHER D. S., *Phys. Rev. Lett.*, **56** (1986) 1964.
- [37] CHAUVE P., LE DOUSSAL P. and WIESE K. J., *Phys. Rev. Lett.*, **86** (2001) 1785 (cond-mat/0006056).
- [38] LE DOUSSAL P., WIESE K. J. and CHAUVE P., *Phys. Rev. B*, **66** (2002) 174201 (cond-mat/0205108).
- [39] LE DOUSSAL P. and WIESE K. J., *Phys. Rev. Lett.*, **114** (2014) 110601 (arXiv:1410.1930).
- [40] MIDDLETON A. A., *Phys. Rev. Lett.*, **68** (1992) 670.
- [41] BAESENS C. and MACKAY R. S., *Nonlinearity*, **11** (1998) 949.
- [42] WIESE K. J., *Phys. Rev. E*, **93** (2016) 042117 (arXiv:1501.06514).
- [43] JANIĆEVIĆ S., LAURSON L., MÅLØY K. J., SANTUCCI S. and ALAVA M. J., *Phys. Rev. Lett.*, **117** (2016) 230601.
- [44] LE DOUSSAL P., MIDDLETON A. A. and WIESE K. J., *Phys. Rev. E*, **79** (2009) 050101(R) (arXiv:0803.1142).
- [45] DORNIC I., CHATÉ H. and MUÑOZ M. A., *Phys. Rev. Lett.*, **94** (2005) 100601.